A LEMP Generator-Simulator Circuit

Un circuito generador-simulador de LEMP

Luis Fernando Díaz Cadavid[1], Eduardo Antonio Cano-Plata[2], Camilo Younes-Velosa[3]

Abstract— **This paper presents a proposal for a LEMP generator-simulator circuit for testing an SDR-detector developed for spectral characterization of lightning, its design and implementation.**

Keywords: **LEMP, SDR, spectral characterization.**

Resumen— **Este artículo presenta una propuesta de un circuito generador-simulador de LEMP para pruebas de un detector tipo SDR desarrollado en la caracterización espectral del rayo atmosférico, su diseño e implementación.**

Palabras claves: **LEMP, SDR, caracterización espectral.**

1. INTRODUCTION

IF there is a natural phenomenon that always affects the quality of energy distributed by the electricity network, it is the electromagnetic pulse generated during the atmospheric lightning discharge, widely known by its acronym LEMP (Lightning Electromagnetic Pulse). This is why, two years ago, three research groups at the Universidad Nacional de Colombia (PAAS - Programa de investigación sobre Adquisición y Análisis de señales, GREDyP - Grupo de Redes de Distribución y electrónica de Potencia and GTT - Grupo de investigación en Telemática y Telecomunicaciones), worked together on a detailed characterization study of LEMP in the central-western part of Colombia (the main coffee-growing area).

One of the goals of these groups consisted of designing and implementing a radio receiver for detecting LEMP and their spectral characterization using Software Defined Radio (SDR) technology.

2. DESIGNING A DEVICE FOR THE SPECTRAL CHARACTERIZATION OF LEMP

Theoretical support: Based on corresponding concepts, the process of lightning generated through a return-stroke discharge channel is interpreted as a transmission system comprising an RF generator having a broadband intermittent pulse wave (equivalent in time and shape to the LEMP) connected at its output to a thin-linear monopole antenna having finite length well below maximum transmission λ and equal to the average height between impacted ground and storm cloud.

The proposed solution: If has been assumed that lightning is a kind of RF transmission system; it thus became necessary to design a radio receiver for detecting signal LEMP. This radio receiver had to enable measuring the parameters needed for supplying the data required for spectral analysis (curve dE/dt) and also had to give the analysis graphically and in terms of power intensity for each frequency component. It is thus proposed to use Software Defined Radio (SDR) technology for this purpose which (although to date has not been explicitly used in this type of receiver) fits more the effective resolution of the stated requirements.

3. LIGHTNING DETECTOR-RECEIVER IMPLEMENTED WITH SDR ARCHITECTURE

A. A basic SDR system

A basic SDR system (Mitola, 1999), consists of a computer (PC) equipped with an Analog-to-Digital Converter (ADC) card, preceded by some form of RF adapter called "Front end" equipment. Significant amounts of signal processing are handed over to the general purpose processor, rather than processed by special-purpose hardware. Such a design produces a radio that can receive different forms of radio protocol or as in the present case, different lightning waveforms, just by running different software (see Figure 1).
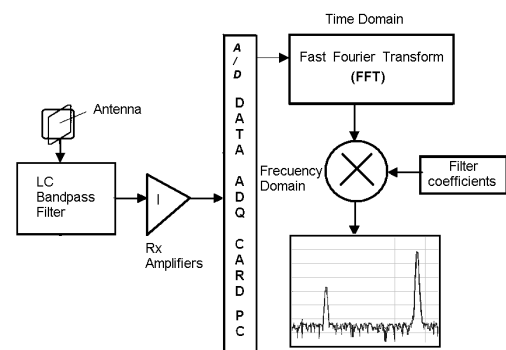

Figure 1. SDR Block diagram

B. The first problem to be solved

Designing and implementing a lightning detector with SDR

1- Master of Science in Telecommunications Engineering, Bonch-Bruevich Saint-Petersburg State University of Telecommunications, Russia. Associate Professor at Universidad Nacional de Colombia. lfdiazc@unal.edu.co

2- Ph.D. in Electrical Engineering, Universidad de Buenos Aires, Argentina. Associate Professor at Universidad Nacional de Colombia. eacanopl@unal.edu.co

3- Ph.D. in Electrical Engineering, Universidad Nacional de Colombia, Colombia. Associate Professor at Universidad Nacional de Colombia. cyounesv@unal.edu.co

technology involves three steps:

1.   Designing and implementing "Front-end" equipment, including antennas, resonant filters, amplifiers, etc;

2.   Specifying the ADC and trigger system in line with the conclusions reached as a result of lightning signal study (object of analysis); and

3.   Designing spectral analysis software carrying digital signal processing: algorithms, digital filters, etc.

Developing each stage requires systematic tests which if possible, are controlled in the laboratory for validating each module's correct functionality. This is where the first problem in the proposed device's design and implementation was presented: the occurrence of lightning in the area of interest is completely unpredictable (i.e. Colombia's coffee-growing area). In other words, there is no continuous or frequent emission signal for verifying proper reception and thereby achieving adequate tuning, and certifying the data so obtained.

Following respective analysis of a possible solution to the first problem, it was found that the most viable and cost-effective one was the design and implementation of a simulation device generating a laboratory-controlled LEMP signal. The proposed solution is presented in this paper as a tested and proved LEMP generator-simulator circuit, as well as its design and implementation.

4.   DESIGNING AND IMPLEMENTING A GENERATOR-SIMULATOR

A. Power requirements

Like an ordinary AM radio receiver, a LEMP SDR-detector, should be able to detect a very low power signal, meaning that the simulator's transmission power requirements can be in the order of milliwatts, regardless of whether the lightning emits a pulse in the order of kilowatts.

B. The emission protocol

As with any transmitter, the emission protocol is referred to or expressed graphically in the signal waveform. In the present case, this means that the simulator must generate a signal having a waveform equal to the LEMP, whilst keeping a temporary proportion.

C. Spectral composition

The signal emitted by the simulator must contain a well defined and controlled complex spectral composition (in terms of frequency and intensity) without unwanted harmonics and without altering the waveform.

Given the above requirements, the design and implementation of the proposed simulation device can be summarized in the following phases:

- Modelling the LEMP signal waveform;
- Modelling the lightning's return stroke vertical channel as an RF transmitting antenna;
- Designing the simulator's electronic circuit;
- Physically assembling the circuit; and
- Testing the device.

5.   MODELLING THE LEMP SIGNAL WAVEFORM

The Figure 2 shows current waveform measured at the lightning return-stroke vertical channel.
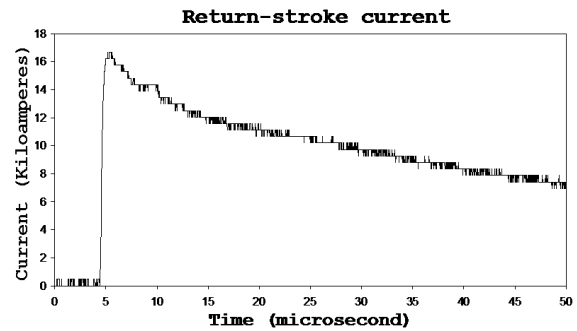

Fig. 2. Waveform of measured current at the vertical lightning return-stroke channel (COST P18, 2009)

This type of waveform is statistically the most common for the LEMP and explains why although the forms of atmospheric wave surges are varied, it has been standardized for pulse testing equipment and electrical machines. A standardized wave is one that has some well-defined characteristics regarding time and form, and in the case of atmospheric overvoltage testing, is specified in IEC (IEC 60060-1/2, 1989) and ANSI standards (ANSI/IEEE Standard 4, 1995).

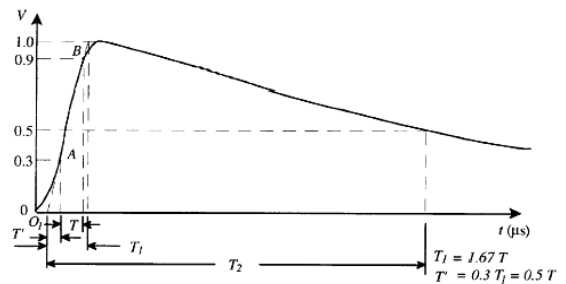Figure 3 shows a full lightning impulse (LI) waveform with definitions for the 1.2/50 μs standard.

Fig. 3. LI 1.2/50 *μ*s (IEC 60060-1) standard with T1-T2 time parameters

Normally, atmospheric lightning impulses are generated in high voltage laboratories using the basic scheme proposed by Erwin Marx in 1924. Years of research have determined that indeed an atmospheric overvoltage can be represented as a unidirectional voltage pulse obtained from circuits such as those proposed in Figures 4a and 4b (Kuffel & Zaengl, 2000):
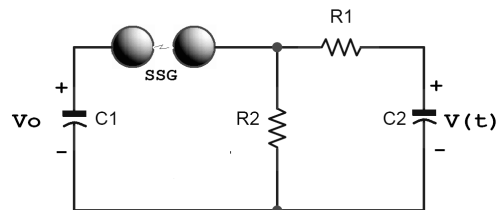

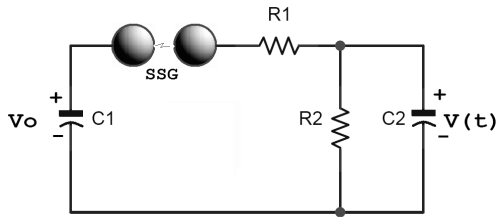Fig. 4a. Pulse generator circuit type A

Fig. 4b. Pulse generator circuit type B

Analysing these circuits showed that capacitor C_1 (representing the pulse generator) was initially charged with DC voltage V_0 (positive or negative polarity), and was then suddenly discharged into a circuit formed by capacitor C_2 and resistors R_1 - R_2. The download began the moment when an electric arc was established between the spheres of spark gap SSG and tension was transferred to C_2, connected in parallel to the object being tested (e.g. a high-voltage electrical transformer).

If switch (SSG) closure were instantaneous and parasitic elements were ignored, this circuit generated a pulse whose time evolution corresponded to a double exponential waveform, where the analytical expression of the voltage pulse on C_2, would be given by (Gallagher and Pearmain, 1973):

$$v_{C_2}(t) = v_0.k.(e^{-\alpha t} - e^{-\beta t}) \qquad (1)$$

Where V_0 is the charging voltage for capacitor C_1, "k" a constant depending on the selected circuit (see Figures 4a and 4b) and α and β the roots of the characteristic equation for the system, whose inverses are its time constants.

If the *resistive* and *capacitive* parameters shown in Figure 4 were constants and α and β values of expression (1) were relatively different, then two circuits could be analyzed separately: the wave-front and the tail, as shown in Figure 5 (Khalifa, 1990):
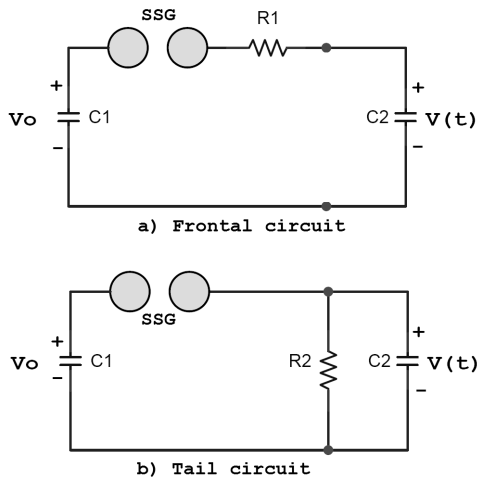

Figure 5. Circuits for analyzing the pulse generator

Considering the wave-front circuit at the time that the discharge occurred between the spheres of spark gap SSG, capacitor C_2 became charged at time T_1:

$$-\frac{1}{\beta} = T_1 = R_1 \frac{C_1 . C_2}{C_1 + C_2} \qquad (2)$$

By a similar process in the tail circuit at the instant when the charge transferred from C_1 to C_2 was zero (due to a redistribution of electric charge between them), the capacitors were discharged into the resistor R_2 with a T_2 time equal to:

$$-\frac{1}{\alpha} = T_2 = R_2(C_1 + C_2) \qquad (3)$$

Analyzing the circuit shown in Figure 4b, from the moment when energy was transferred between capacitor C_1 and capacitor C_2, gave the following equation in the frequency domain (Laplace transform):

$$V_{(S)} = \frac{V_0}{K} \frac{1}{\left(S^2 + a.S + b\right)} \qquad (4)$$

where: S - was the complex angular frequency, $k = R_1 C_2$ and

$$a = \left(\frac{1}{R_1 C_1} + \frac{1}{R_1 C_2} + \frac{1}{R_2 C_2} \right) \qquad (5)$$

$$b = \left(\frac{1}{R_1 R_2 C_1 C_2} \right) \qquad (6)$$

The equation in the time domain would mean that voltage on the capacitor C_2 (pulse generator output) would be:

$$v_{(t)} = \frac{v_0}{k} \frac{1}{(\alpha_2 - \alpha_1)} (e^{-\alpha_1 t} - e^{-\alpha_2 t}) \qquad (7)$$

where,

α_1 and α_2 were the roots of the equation: $\mathbf{S^2 + (a*S) + b = 0}$

$$\frac{1}{\alpha_1} = \frac{2}{a + \sqrt{a^2 - 4b}} \quad , \quad \frac{1}{\alpha_2} = \frac{2}{a - \sqrt{a^2 - 4b}} \qquad (8)$$

or

As the voltage in C_2 was $V_{(t)}$, and was the superposition of two exponential functions of different signals, according to (8), the negative response of the root was a larger time constant ($1/\alpha_1$), than the positive time ($1/\alpha_2$). The graph in Figure 6 represents expression (8), from which the following could be defined:

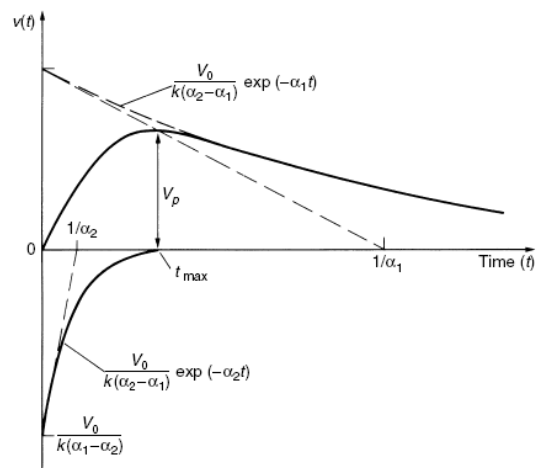$$\alpha_1 + \alpha_2 = a \quad \text{and} \quad \alpha_1.\alpha_2 = b \qquad (9)$$

Figure 6. Voltage impulse wave and its components

For the type B circuit shown in Figure 4b, using (9) and

substituting the values of ***a*** and ***b*** in (5) and (6), one could calculate the values for resistors R1 and R2 as follows:

$$R_1 = \frac{1}{2C_1}\left[\left(\frac{1}{\alpha_1}+\frac{1}{\alpha_2}\right)-\sqrt{\left(\frac{1}{\alpha_1}+\frac{1}{\alpha_2}\right)^2-\frac{4(C_1+C_2)}{\alpha_1\alpha_2.C_2}}\right] \quad (10)$$

$$R_2 = \frac{1}{2(C_1+C_2)}\left[\left(\frac{1}{\alpha_1}+\frac{1}{\alpha_2}\right)+\sqrt{\left(\frac{1}{\alpha_1}+\frac{1}{\alpha_2}\right)^2-\frac{4(C_1+C_2)}{\alpha_1\alpha_2.C_2}}\right] \quad (11)$$

Following analysis of the circuit shown in Figure 4b, it was noted that time t_1 (front time) taken to load C_2 through R_1, would be approximately:

$$t_1 = 3.R_1.\frac{C_1.C_2}{C_1+C_2} \quad (12)$$

In the same way for determining the tail time, it was observed that both capacitors C_1 and C_2 were discharged through R1 and R2, so the time taken to 50% of download was approximately:

$$t_2 = 0.7(R_1 + R_2)(C_1 + C_2) \quad (13)$$

6. MODELLING LIGHTNING RETURN STROKE VERTICAL CHANNEL AS AN RF TRANSMITTING ANTENNA

Lightning return-stroke models are needed when studying lightning effects on various systems and in characterizing the lightning electromagnetic environment (Betz *et al.*, 2009). Return-stroke models have been categorized into four classes based on governing equations (Rakov and Uman, 2006): gas dynamic models, electromagnetic models, distributed-circuit models and "engineering" models.

Electromagnetic models are based on a lossy, thin-wire antenna approach to the lightning return-stroke channel. Lightning discharge is a thin channel when compared to its overall length (it was determined that average return-stroke channel radius is 1–2 cm). There is usually great interest in the electromagnetic fields radiated by LEMP several kilometers away. Hence, the return-stroke channel is modelled as a linear antenna for calculating electric and magnetic fields generated by LEMP, which have some current distribution or which have a certain line charge density distribution that changes as time elapses. Besides, lightning discharge is self propagating and its length extends at great speed, sometimes at a significant fraction of the speed of light (1-2x10^8 m/s). Field calculations must thus bear in mind retardation due to signal's finite travel time at the speed of light (Cooray, 2008).

According to Y. Baba and V. Rakov (Betz *et al.*, 2009), the most general equations for computing vertical electrical field E_Z and azimuth magnetic field B_φ due to an upward-moving return stroke are given by Rajeev Thottappillil (Thottappillil *et al.*, 1997). However, those equations are "time-domain" expressions applicable to any line source distribution varying with time, since LEMP is a transient event non-periodically changing its current and charge distribution in space and time. But, if one wishes to remodel the return-stroke channel as an

RF transmitter, taking into account that the goal is to obtain a spectral LEMP characterization, this may be done by simulating the lightning discharge channel as a vertical thin-wire monopole antenna, excited at its base by an EMP generator, and look for expressions of electric and magnetic fields radiated by an electric dipole in the frequency domain.

Let us see:

Figure 7 shows a graphical model of such antenna with length L equal to the height of the storm cloud, excited at its base by an EMP generator.

If magnetic potential were calculated at point P (ρ, Φ, z) then the electric and magnetic field could be known at that point.

In (Schelkunoff and Friis, 1952; Jordan and Balmain, 1968; Weeks, 1968) have been given a complete development of these fields; Figure 7 shows results in cylindrical coordinates. Here:

Given the vector's magnetic potential (delayed) at point P:

$$[A_z] = \frac{\mu I_{max}}{4\pi}\left[\int_0^L \frac{sen(\beta(L-z))e^{-j\beta D}}{D}dz + \int_{-L}^0 \frac{sen(\beta(L+z))e^{-j\beta D}}{D}dz\right] \quad (14)$$

Where: $I = I_{max}\,sin\,(L-z)$ for $z > 0$

$I = I_{max}\,sin\,(L+z)$ for $z < 0$

L = Monopole length in meters.

λ = Length wave

$\mu_0 = 4\pi \times 10^{-7}$ [Henries/meter] = Vacuum permeability.

$\beta = 2\pi/\lambda$ [rad/m] = Propagation constant.

$r = \sqrt{Z^2+Y^2}$, $D = \sqrt{(Z-z)^2+Y^2}$

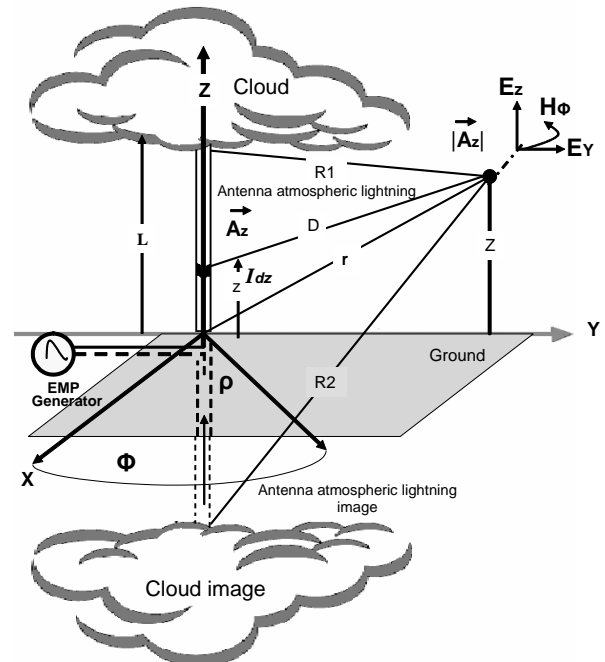$R_1 = \sqrt{(Z-L)^2+Y^2}$ $R_2 = \sqrt{(Z+L)^2+Y^2}$

Figure 7. Model of lightning return-stroke channel as vertical monopole antenna

Given that the element of current in the antenna had direction Z and the magnetic field had direction Φ, then a single component was reached for solving rotor A_Z, i.e.:

$$H_\Phi = \frac{1}{\mu}(\nabla x A_Z)_\Phi = -\frac{1}{\mu}\frac{\partial A_Z}{\partial \rho} \qquad (15)$$

As the magnetic field was orthogonal to the antenna (power source) one could take point P without loss of generality in the ZY plane (plane X = 0) therefore:

$$H_\Phi = -\frac{1}{\mu}\frac{\partial A_Z}{\partial Y} \qquad (16)$$

Leading to:

$$H_\Phi = \frac{j30I_{max}}{\eta Y}\left(e^{-j\beta R_1} + e^{-j\beta R_2} - 2\cos(\beta L)e^{-j\beta r}\right) \qquad (17)$$

The expression (17) shows that the magnetic field could be calculated at any point in space (near and far field).
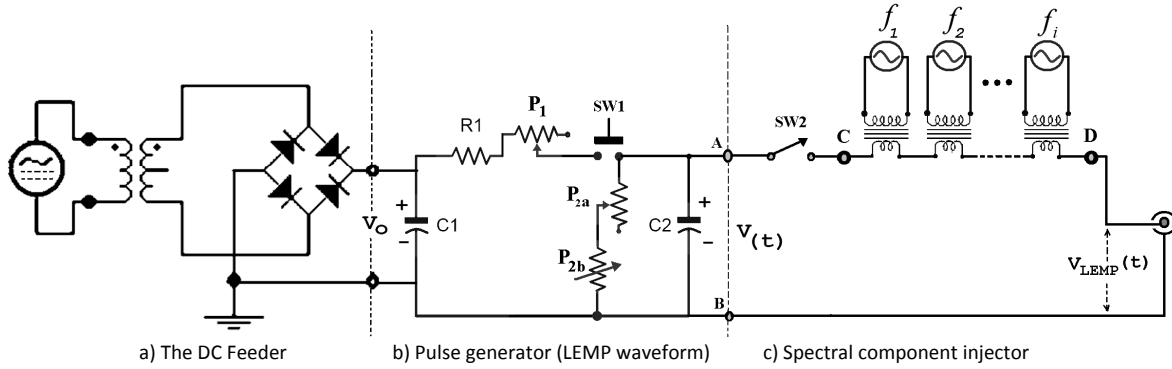

a) The DC Feeder   b) Pulse generator (LEMP waveform)   c) Spectral component injector
Figure 8. Proposed LEMP generator-simulator circuit

Two electric fields, E_Z and E_Y where obtained when solving the rotor for the H_Φ field:

$$E_Z = -j30I_{max}\left(\frac{e^{-j\beta R_1}}{R_1} + \frac{e^{-j\beta R_2}}{R_2} - 2\cos(\beta L)\frac{e^{-j\beta r}}{r}\right) \qquad (18)$$

$$E_Y = j30I_{max}\left(\frac{z-L}{Y}\frac{e^{-j\beta R_1}}{R_1} + \frac{z+L}{Y}\frac{e^{-j\beta R_2}}{R_2} - 2\frac{z}{Y}\cos(\beta L)\frac{e^{-j\beta r}}{r}\right) \qquad (19)$$

As the magnetic field (17) expressions (18) and (19) allowed electric fields in every region of space to be calculated, then I_{max} (maximum current distribution value) either simulated or real, was given, obtained by the right equipment.

The data for variables r, R_1 and R_2 could be obtained by measuring the D-parameter, if the geographic location of the measurement and impact site were known.

Up to this point the expressions were obtained by using a constant β depending on a λ related to a single frequency, but it is necessary to consider that the LEMP is a signal with a complex RF spectrum.

It should be remembered that RF radiation by lightning discharges has been studied during recent decades in various frequency ranges (Weidman *et al.*, 1981; Levine, 1986; Upul *et al.*, 2006) and has determined that "I_{max}" current shows a broadband spectral composition which is important characterize, for the adjustment corresponding to each field calculation.

With this new argument, the model had to be redesigned and lightning discharge channel interpreted as a transmission system consisting of an RF generator formed by an array of multiple sine wave oscillators in parallel and connected at its output to a thin-linear monopole antenna having finite length

well below maximum transmission λ and equal to the average height between impacted ground and storm cloud. Every oscillator would be a source of sine current given by:

$$I(f_i) = A_i sin(2\pi f_i t + \Phi_i)\text{ [Amp]} \qquad (20)$$

Where A_i was the amplitude of the "**i**-source" proportionally equivalent in time and shape to the LEMP and f_i was the frequency for each independent current generator.

Using the above concepts and taking **η** (characteristic impedance of free space) as **η** =120π [Ω], new expressions were obtained for (17)-(19), thus:

$$H_\Phi = \sum_{i=1}^{n}\frac{jI(f_i)}{4\pi}\left(\frac{e^{-j\beta_i R_1}}{Y} + \frac{e^{-j\beta_i R_2}}{Y} - 2\cos(\beta_i L)\frac{e^{-j\beta_i r}}{Y}\right) \qquad (21)$$

$$E_Z = \sum_{i=1}^{n}-j30I(f_i)\left(\frac{e^{-j\beta_i R_1}}{R_1} + \frac{e^{-j\beta_i R_2}}{R_2} - 2\cos(\beta_i L)\frac{e^{-j\beta_i r}}{r}\right) \qquad (22)$$

$$E_Y = \sum_{i=1}^{n}j30I(f_i)\left(\frac{z-L}{Y}\frac{e^{-j\beta_i R_1}}{R_1} + \frac{z+L}{Y}\frac{e^{-j\beta_i R_2}}{R_2} - 2\frac{z}{Y}\cos(\beta_i L)\frac{e^{-j\beta_i r}}{r}\right) \qquad (23)$$

If it were assumed that the proposed LEMP receiver with SDR technology was able to detect all spectrum components with their power intensities and if care was taken to measure these intensities at the same time "*t*", then it could be presumed that the overall power of LEMP (P_{LEMP}), would be equal to:

$$P_{LEMP} = \sum_{i=1}^{n}P(f_i)\quad[w] \qquad (24)$$

7. DESIGNING THE SIMULATOR ELECTRONIC CIRCUIT

The proposed simulation circuit can be divided into three functional modules (see Figure 8):

- The DC feeder;
- Pulse generator (with LEMP waveform); and
- spectral component injector (AM modulator)

A. The DC feeder

A pulse generator for testing electrical transformers normally feeds from a DC kilovolts source obtained by rectifying the AC waveform present at the output of a transformer controlled by a variable voltage (Variac). However, in present case, an AC/DC conventional converter or a full-wave rectifier was used in its place since the power requirement was given in the order of milli-watts, giving small 5 VDC or 12 VDC voltages (see Figure 8.a.).

B. Pulse generator (with LEMP waveform)

To generate a pulse equivalent in time and shape to the LEMP and similar to the standard pulse used to test transformers, it was proposed using an adaptation of the B circuit shown in Figure 4b.

A fast tact switch (SW1) was used in the proposed circuit (see Figure 8.b.) instead of a switch of sphere gap (SSG); this was installed between R1 and R2 || C2. Besides, one Multi-turn cermet trimmer potentiometer (P1) was added in series with R1 for providing the user with manoeuvrability and control of front time "t1", in the same way, R2 was replaced by a Multi-turn cermet trimmer potentiometer P2a in series with a control potentiometer P2b for to management the tail-time "t2". Thus, the calculations for t_1 and t_2 formulated in (12) and (13), remained as follows:

$$t_1 = 3(R_1 + P_1)\frac{C_1.C_2}{C_1+C_2} = 3(R_1 + P_1)C_e \qquad (25)$$

$$t_2 = 0.7\left[(R_1+P_1)+(P_{2a}+P_{2b})\right](C_1 + C_2) \qquad (26)$$

Where if (R_1+P_1) is expressed in ohms and $C_e=(C_1.C_2)/(C_1+C_2)$ in microfarads, then t_1 is obtained in microseconds.

It is known that C1 >> C2 is needed to achieve good generator performance (or relationship between the peak pulse voltage and DC load voltage, V_0) and that R1 <<R2 to achieve lightning waveform or as in present case, (R1 + P1) << (P2a + P2b).

Such conditions would lead to: $C_1+C_2 \approx C_1$ and $[(R1+P1)+(P_{2a}+P_{2b})] \approx (P_{2a}+P_{2b})$ with which (25) and (26) could be simplified, obtaining:

$$t_1 \cong 3(R_1 + P_1)C_2 \qquad (27)$$

This would indicate that capacitor C2 wave front voltage length was directly proportional to the front resistance (R1 + P_1) and the module connected in parallel to C2 and

$$t_2 \cong 0.7(P_{2a} + P_{2b})C_1 \qquad (28)$$

This would indicate that tail time proportionally depended on tail resistance ($P_{2a}+P_{2b}$) and capacitance C1.

It should be noted that once desired values for t1 and t2 had been specified and the values given for C1 and C2, it was possible to establish (at least regarding a first approximation) the required values of R1 and R2, for obtaining the desired waveform in the LEMP proposed simulator's output.

C. Spectral component Injector (AM modulator)

As non-standard waveform had already been obtained, it then became necessary to inject a spectral frequency composition without altering the waveform to achieve a similar wave to real LEMP.

According to the model, this spectral composition was generated because the lightning antenna was excited at its base by an array of parallel coupled oscillators. However, it is well known that when voltage sources (frequency generators) are connected in parallel in practice then feedback currents are produced which can damage these devices. Furthermore, sources connected in parallel must adjust their output to maintain zero current imbalance. This raises a problem in the case of wanting to literally apply this model to developing the proposed device.

To overcome this design problem, the proposed solution was very simple; an inductive coupling was made by connecting each frequency generator to a signal transformer on its higher impedance coil side (thereby acting as primary coil) and by connecting these transformers' "secondary coils" in series, following the circuit diagram proposed in Figure 8.c. Specific sinusoidal currents were thus induced on the wave emitted by the proposed pulse generator, thereby obtaining a kind of AM modulation where as carrier signal would act the simulated pulse (supplied by the generator) having an amplitude **A**, varying at time and equal to **V(t)**, and frequencies emitted by the generators would act as modulators induced by signal transformers. The voltage of the simulated lightning signal so obtained with the proposed circuit, called $V_{LEMP}(t)$, would thus be given by:

$$V_{LEMP}(t) = v(t) + \sum_{i=1}^{n} A_i \sin 2\pi f_i t \qquad (29)$$

Where:

f_i - was the frequency emitted by generator **i**-th, and

A_i – was the amplitude induced by frequency generator **i**-th which would be given by:

$$A_i = K_i a_i \ [V_{DC}] \qquad (30)$$

Where K_i **was** a constant of proportionality (transfer rate) given by the transformer T_i and a_i was the amplitude set by the user for each **i**-th frequency generator.

8. PHYSICALLY ASSEMBLING THE CIRCUIT

An old DVD player was used for assembling the circuit, using the chassis, the power module (providing us with high

stability +5, -5, +12 and -12 VDC power feed values), the "fast contact switches" and the volume potentiometer (control P) from the front panel (to cut financial costs).

The following relationships were maintained for C1, C2, R1, P1, P2a and P2b values:

1. $C_1 \gg C_2$ 2. $(R_1+P_1) \ll (P_{2a}+P_{2b})$

Two electrolytic capacitors values could be C1= 470 µF and C2= 4.7 µF considering a 100>>1 ratio which can be easily found in unusable radio receivers.

Other elements which are available from unusable radio receivers and fax modem cards (obsolete) are the signal transformers.

BNC standard connectors were used as input/output points.

The following tips should be considered during assembly:

a) Frequency generators input points should not have any contact in common, to avoid feedback currents (look for isolated ground);

b) When connecting signal transformers, the greater resistance coil must be connected to the frequency generator (current source), contrary to usual practice in voltage transformers.

c) For proposed circuit, primary coil's ohm resistances must have a much greater value than secondary coil resistance and these secondary coils must have a very low value (2 - 30 Ω) to ensure that induced voltages do not affect the waveform;

d) To get the best frequency range, the low impedance side of the signal transformer must be put in series with the others; and

e) As the frequency response of each signal transformer used depends on the transfer ratio, its design and construction materials, it is very important to carefully determine their bandwidth to avoid unwanted harmonic generation. This data must be recorded as part of the device's specifications and technical information for the end user.

If it is desired to add radio emitter functionality to the proposed device to perform radio-detection tests, then an amplifier module would have to be appended to the LEMP generator output, connected to a broadband antenna.

Figure 9 shows a photo of the proposed device assembled in the chassis and connected to three frequency generators on its input side and to a spectrum analyzer with 9 kHz - 3 GHz bandwidth in the output.

Fig. 9. A photo of the "LEMP Generator-Simulator" in a performance test

9.   PERFORMANCE TEST

A. Generated waveform test

A Fluke 199C (200 MHz bandwidth and 2.5 Gs/s) ScopeMeter was connected at points A and B of the circuit (see Figure 8) so that the equipment did not generate any signal in idle mode. Once the P2b potentiometer had been adjusted (via a knob located on the front of the device) to its minimum position (P2b = 0 Ω), and the SW1 button pressed, the graph shown in Figure 10 was obtained.
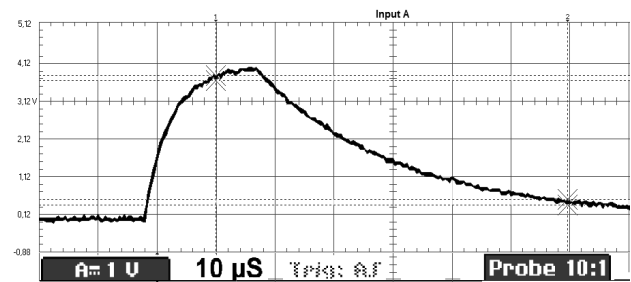

Figure 10. Generated LI wave-shape with a P1↑ and P2b↓

Then, using a precision screwdriver, the P1 value was changed to its minimum and SW1 pressed again, leading to wave front-time change, as recorded in Figure 11 (here the wave presents a "front-time" similar to "standard wave front-time").
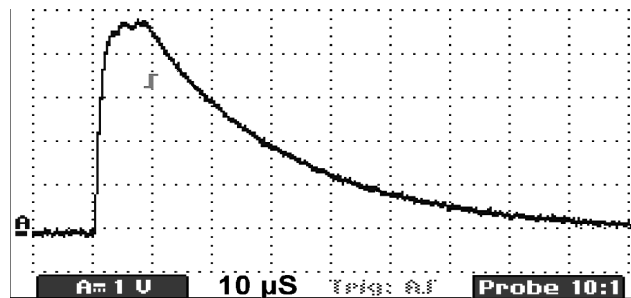

Figure 11. Generated LI wave-shape with a P1↓ and P2b↓

Then P2b value was then changed to obtain its maximum resistance value, and SW1 was pressed to change the "tail-time" of the pulse. At this point the pulse waveform had already acquired the desired shape (see Figure 12) and SW1

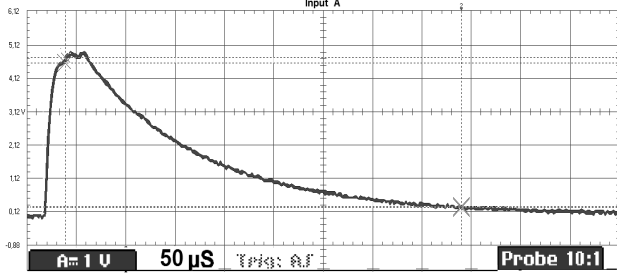had been pressed as quickly as possible.

Figure 12. LI wave-shape with P1↓ and P2b↑↑

When pressing the SW1 switch slower it was observed that pulse fall time became extended, as shown in Figure 13.
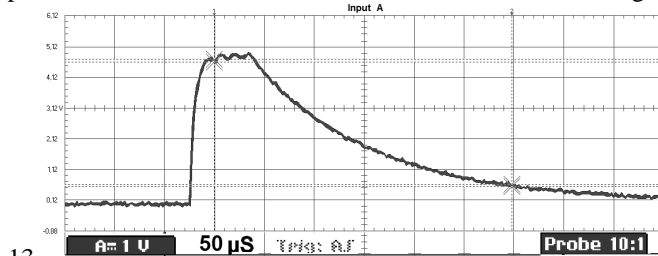

Figure 13. LI wave-shape with t_3↑↑

B. Spectrum injector Test

The SW2 switch was put in the "open" position (see Figure 8) and a DSA1030 RIGOL spectrum analyzer (BW 9 kHz - 3 GHz) was connected to the points C and D on the circuit. The three frequency generators linked to the device were given the following values: F1 = 100 kHz, F2 = 200 kHz and F3 = 900 KHz. It was observed that these frequencies were indeed those recorded by the spectrum analyzer (see Figure 14) and that no other frequency was detected.

Frequency values were then changed (F1 = 10 kHz, F2 = 100 kHz and F3 = 1000 kHz) as were generator output amplitudes (Ai) and the resulting data were recorded for comparison with data obtained using other equipment for spectrum analysis, in this case with a Fluke ScopeMeter, in spectrum analyzer mode (see Figure 15).
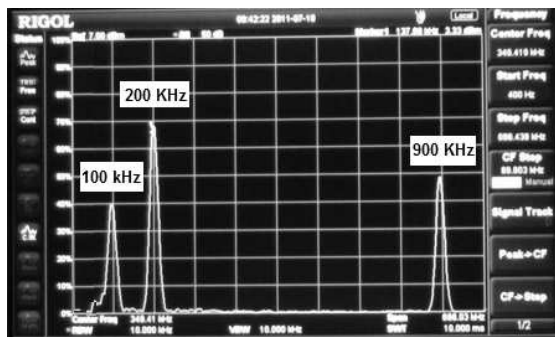

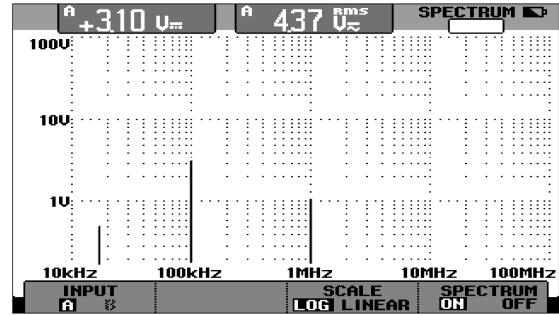Figure 14. Spectrum analyzer display showing the detected frequencies

Figure 15. Spectrum analyzer display showing the detected frequencies

C. Final simulated LEMP Generator Test

SW2 was put in the "closed" position and a new spectrum analyzer (PC DSO 2100) connected to the proposed device's output connector. By repeatedly pressing SW1 was observed that the analyzer was recording the same frequencies injected (see Figure 16) only this time there was a high DC component power intensity (F = 0 Hz).
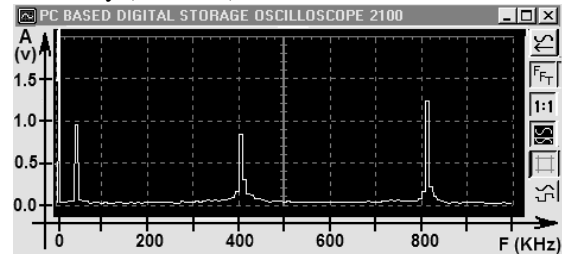

Figure 16. Spectrum analyzer display (DSO-2100) showing detected frequencies: F1, F2, F3 and DC component.

A Fluke ScopeMeter (in Oscilloscope mode) was then connected to the device's output connector, and SW1 was pressed to achieve a pulse similar to the "standard pulse" but with spectral composition which was more like real LEMP (see Figure 17).

10. TEST ANALYSIS

The fact that when the device was in "Power-On" state and no signal was present before pressing SW1 (pulse start time) guaranteed the absence of "noise" causing distortion of the signal being studied.
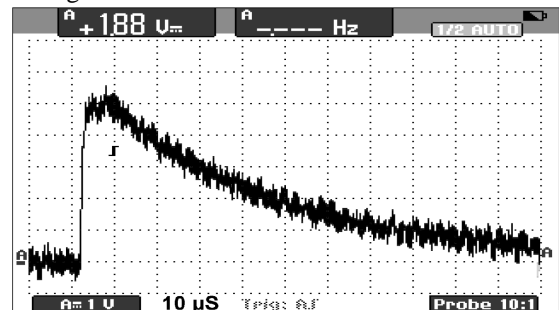

Figure 17. ScopeMeter display showing waveform likeness to real LEMP

The change in P1 value was reflected in pulse front-time (see Figures 10 and 11), thereby demonstrating the relationships expressed in (25) and (27).

The change of P2b value was reflected in pulse tail-time (see Figures 10 and 12), demonstrating the relationships

expressed in (26) and (28).

The delay in the time for pressing SW1 also lengthened C2 charging time and prolonged the wave tail. Then time $t2$ in expression (28) for this LEMP generator-simulator, also considering that the relationship remained C1>> C2, would be given by:

$$t_2 \cong 0.7(P_{2a} + P_{2b})C_1 + t_3 \qquad (31)$$

Where: t_3 was the contact time taken by pressing SW1.

The idea was to carry t_3 to a value very close to 0 ($t_3 \rightarrow 0$). However, this would have required another kind of switch (e.g. opto-electronic), thereby increasing the cost of assembling the device, this being unnecessary in view of the design objectives for the device in question.

It can be said that the waveform obtained (see Figure 17) met the design objectives, given its resemblance to the 1.2/50 µs form of a standard impulse wave.

11.   CONCLUSIONS

A circuit for generating "*simulated LEMP*" has been presented to the scientific community as a small contribution towards research into lightning's spectral characteristics.

The device allowed a user to control wave front/tail times in addition to injection frequencies and their intensities, thereby providing versatility regarding the possibilities offered concerning waveform and spectral composition.

When comparing Figure 2 with Figure 17 it can be concluded that the device offers a LEMP really close to that of the real one.

Given that this LEMP generator-simulator emitted a pulse having controlled spectral composition (the user chooses the frequencies and intensities), then this device would allow testing the proper operation of any lightning detector using resonant tank techniques.

It can thus be said that this circuit represents one more useful tool for validating whether spectral analysis software algorithms (or methods) are effective in defining whether detected frequencies are real or are "spectral leakages" produced by the mathematical procedures so applied.

12.   REFERENCES

ANSI/IEEE Standard 4-U.S.A, "IEEE Standard Techniques For High Voltage Testing", 1995.

Betz, H. E., et al (eds.), Lightning: Principles, Instruments and Applications, (Springer, Munich, 2009).

Cooray, V., "The lightning flash", Institution of Engineering and Technology, London, United Kingdom, 2008.

COST P18: The Physics of Lightning Flash and Its Effects, 2009, Available: http://www.costp18-lightning.org/

Gallagher, T., Pearmain, A., High voltage. Measurement, testing and design, John Wiley & Sons, 1973.

IEC 60060-1:1989, High Voltage Test Techniques" – Part 1 "General definitions and test requirement" published by the International electrotechnical Commission.

Jordan, E. C., Balmain, K. G., Electromagnetic Waves and Radiating Systems, Second Edition, Prentice Hall, Inc., 1968.

Khalifa, M., "High-Voltage Engineering Theory and Practice", Marcel Dekker, Inc, 1990.

Kuffel, E., Zaengl, W., High Voltage Engineering Fundamentals, Butterworth, 2000.

Levine, D. M., "Review of Measurements of the RF Spectrum of Radiation from Lightning", NASA Technical Memorandum 87788, 1986.

Mitola, J., "The Software Radio", IEEE Journal on selected areas in communications, vol. 17, no. 4, pp. 514-538, abril 1999.

Rakov, V.A., Uman, M.A., LIGHTNING, Physics and Effects, Cambridge University Press, New York, 2006.

Schelkunoff, S. A., Friis, H. T., Antennas Theory and Practice, John Wiley & Sons, 1952.

Thottappillil, R., Rakov V. A., Uman, M. A., "Distribution of charge along the lightning channel: relation to remote electric and magnetic fields and return-stroke models", J. Geophysics, Res., 102:6987-7006, (1997).

Upul, S., Vernon, C., Mahendra, F., "The lightning radiation field spectra of cloud flashes in the interval from 20 kHz to 20 MHz", IEEE Trans. on Electromagnetic Compatibility, Vol. 48, No. 1, Feb. 2006, pp. 234-239.

Weeks, W. L., Antenna Engineering, McGraw-Hill, Nueva York, 1968.

Weidman, C. D., Krider, E. P., Uman, M. A., "Lightning Amplitude Spectra in the Interval From 100 kHz to 20 MHz", Geophys. Res. Lett., -8, 1981, pp. 931-34.